Chapter 8

Introduction to geometric and kinematic modeling of parallel robots

8.1. Introduction

Parallel architectures were originally proposed in the context of tire-testing machines and flight simulators [Gough 56], [Stewart 65]. Since then, they have been used in other applications requiring manipulation of heavy loads with high accelerations such as vehicle driving simulators or the riding simulator developed for the French National Riding School.

Recently, these kind of structures have attracted considerable interest in various manufacturing applications due to their inherent characteristics, as compared with those of serial robots, which include high structural rigidity and better dynamic performances. This concept is currently used in designing new generations of high speed machine tools.

This chapter deals with the geometric and kinematic modeling of such robots. It is shown that the closed-form solution of the inverse geometric model is straightforward for a six degree-of-freedom parallel robot. The explicit formulation of the direct geometric model is usually more complicated since it can have up to 40 solutions [Husty 96]. Similarly, the computation of the inverse kinematic model is easier than the computation of the direct kinematic model.

8.2. Parallel robot definition

A parallel robot is composed of a *mobile platform* connected to a *fixed base* by a set of identical parallel kinematic chains, which are called *legs*. The end-effector is fixed to the mobile platform. A parallel robot is said to be *fully parallel* when the number of legs is greater or equal to the number of degrees of freedom of the mobile platform, each parallel chain having a single actuator [Gosselin 88]. For example,

Figures 8.1 and 8.2 show a six degree-of freedom fully parallel robot where the mobile platform and the base are linked together by six legs. The desired mobile platform location can be obtained by changing the leg lengths using actuated prismatic joints. This architecture has been used by Gough in 1947 to design tire-testing machines and has inspired Stewart [Stewart 65] to design a flight simulator. It is known as the Gough-Stewart parallel robot.

Note that a *hybrid parallel robot* is formed by a series of several parallel robots. The advantage of such a structure is to increase the workspace of the terminal platform. Figure 8.3 shows the Logabex hybrid robot [Charentus 90], which is composed of four units of parallel structures.

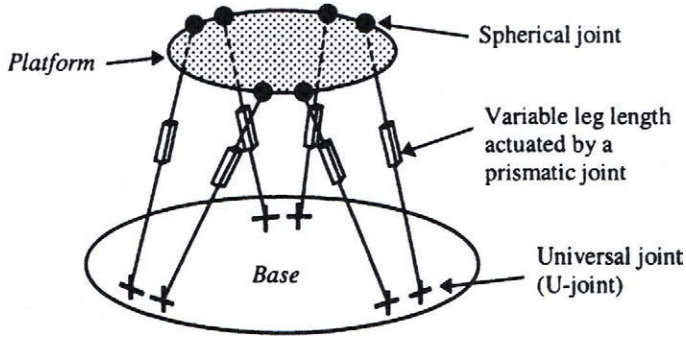

Figure 8.1. *A six degree-of-freedom parallel robot*

8.3. Comparing performance of serial and parallel robots

The main criteria for comparing performance of serial and parallel robots are the workspace, the ratio between the payload and the robot mass, the accuracy, and the dynamic behavior:

i) workspace. The main drawback of a parallel robot is its comparatively small workspace. It is determined by the intersection of the workspaces of all the parallel kinematic chains;

ii) payload - robot mass ratio. In a serial architecture, the end-effector and the manipulated object are located at the extremity of the mechanical chain. Consequently, each actuator must have the necessary power to move not only the object, but also the links and actuators in between. This leads to a poor payload - robot mass ratio.

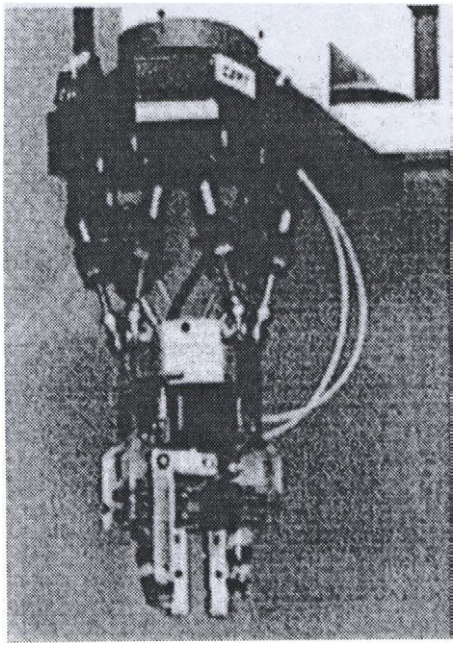

Figure 8.2. *The SPACE-1 parallel robot from CERT (courtesy of CERT)*

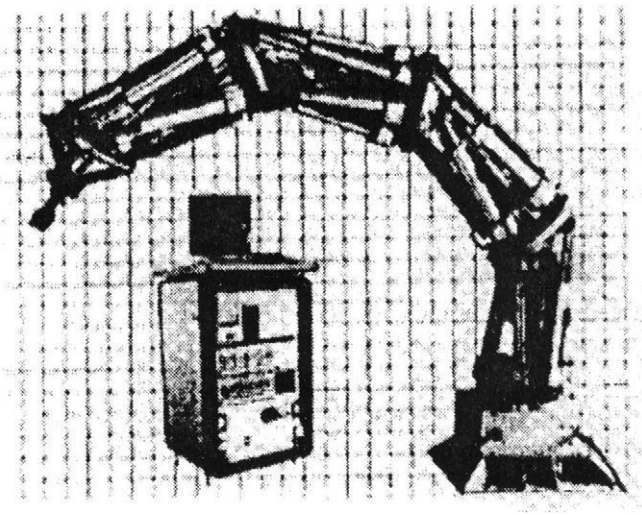

Figure 8.3. *Logabex robot, LX4 model*

In parallel structures, the load is directly supported by all the actuators. Besides, the actuators can be located either on or close to the base. Therefore, the links between the mobile platform and the base can be lightened considerably, and the payload - robot mass ratio is much higher, generally with a factor of at least 10;

iii) accuracy and repeatability. Serial robots accumulate errors from one joint to the next, since defaults like clearance, friction, flexibility, etc. also act in a serial manner. Moreover, the influence of a joint default on the end-effector location is larger when the joint is close to the robot base.
Parallel robots do not present this drawback and their architecture provides a remarkable rigidity even with light connecting links;

iv) dynamic behavior. Considering their high payload - robot mass ratio and their reduced coupling effect between joints, parallel robots have better dynamic performance.

8.4. Number of degrees of freedom

A parallel manipulator is a complex closed loop structure. We recall that computing the number of degrees of freedom of a closed structure using classical formulas (§ 7.10) that do not take into account the geometric constraints may give wrong results. Nevertheless, the number of degrees of freedom of a parallel robot N can be determined using the following simple relationship, which is derived from equation [7.57] and proved to be true for a large number of architectures:

$$N = \sum_{i=1}^{L} m_i - \sum_{j=1}^{B} c_j \qquad [8.1]$$

with:

- B: number of independent closed loops, equal to $(n_c - 1)$, where n_c is the number of parallel chains;
- m_i: mobility of joint i;
- L: total number of joints;
- c_j: number of constraints of the j^{th} loop. In general, $c_j = 3$ for a planar loop, $c_j = 6$ for a spatial loop.

If the kinematic chains between the base and the mobile platform are identical and if the loops have the same number of constraints, equation [8.1] becomes:

$$N = n_c\, d - c_j\, B \qquad [8.2]$$

where d is the sum of the degrees of freedom of the joints in a chain and c_j indicates the number of constraints per loop.

For non-redundant robots, N gives the number of degrees of freedom of the mobile platform with respect to the base.

8.5. Parallel robot architectures

Practically, two classes of parallel robots may be distinguished: planar robots and spatial robots. In this section, we present both classes as well as a specific family of spatial robots: the *Delta robots*.

8.5.1. *Planar parallel robots*

A planar robot is composed of a mobile platform with three degrees of freedom with respect to the base: two translations and one rotation about the normal to the plane of the mobile platform (Figure 8.4). In accordance with the definition of the fully parallel robot, the mobile platform is connected to the base by three legs, each including an actuated joint.

The number of independent loops B of the planar robots of Figure 8.4 is two. If we assume that the three legs are identical, the application of equation [8.2] leads to:

$$N = 3d - 6 \qquad [8.3]$$

From equation [8.3], we deduce that, for N = 3, the number of degrees of freedom d of a leg must be three (two passive and one active).

Let A_1, A_2 and A_3 be the connection points of the base with the legs and B_1, B_2 and B_3 be the connection points of the legs with the mobile platform. To control the position and the orientation of the mobile platform, we have to change the length of the A_iB_i legs. The following three architectures are possible for the legs:

- R-P-R architecture (Figure 8.4a), which is actuated by the prismatic joint;
- P-R-R architecture (Figure 8.4b), which is actuated by the prismatic joint;
- R-R-R architecture (Figure 8.4c), which is actuated by the revolute joint close to the base.

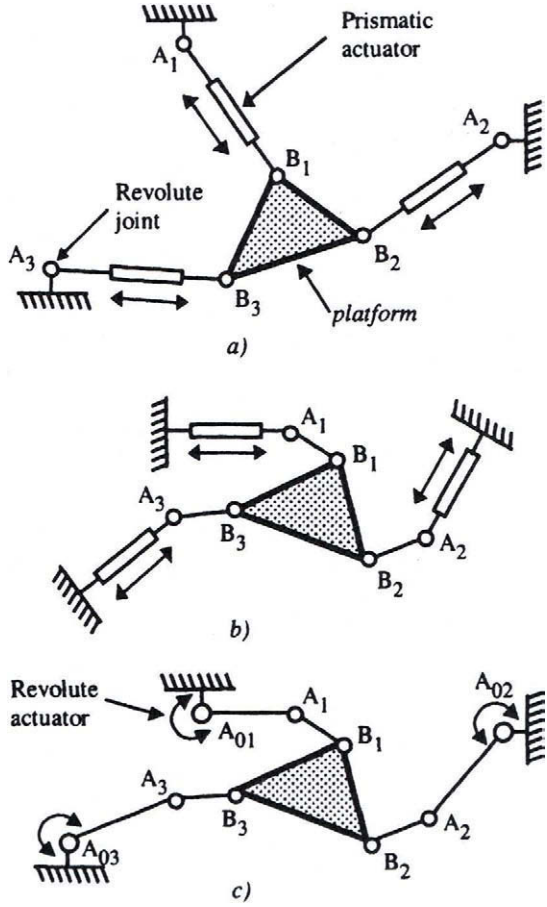

Figure 8.4. *Examples of planar robot architectures*

8.5.2. *Spatial parallel robots*

In general, the mobile platform of spatial robots can have either three degrees of freedom to place a point in the space or six degrees of freedom to place the end-effector at any arbitrary location. To determine the type of joints of each leg, we proceed as for planar robots while assuming that the legs are identical.

8.5.2.1. *Three degree-of-freedom spatial robots*

The mobile platform is connected to the base by three legs. There are two independent loops, and equation [8.2] yields:

$$N = 3d - 12 \qquad [8.4]$$

Since N = 3, the number of degrees of freedom d of each leg must be five (four passive and one active). The passive degrees of freedom can be distributed according to the combinations (0,4), (1,3) or (2,2).

The (1,3) combination is the most commonly used. It is composed of a revolute joint at one end and a spherical joint (RRR) at the other. Figure 8.5a depicts such an example, where the leg length is actuated by a prismatic joint, giving for each leg an R-P-(RRR) architecture. Figure 8.5b gives an example of the (0,4) combination, where the four degree-of-freedom joint is constructed with two universal joints (RR). Each leg is actuated by a revolute joint fixed on the base and presents an R-(RR)-(RR) architecture.

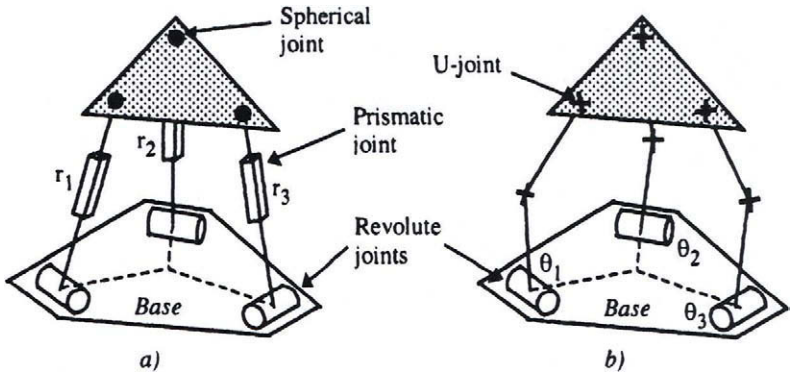

Figure 8.5. *Three degree-of-freedom spatial robots*

8.5.2.2. *Six degree-of-freedom spatial robots*

We consider the Gough-Stewart structure as representative of the six-degree-of-freedom spatial robots. Merlet [Merlet 00] describes three concepts of six degree-of-freedom architectures where the base and the mobile platform are connected by six legs driven by prismatic actuated joints (Figure 8.6):

- *SSM robot (Simplified Symmetric Manipulator)* in which the base and the mobile platform are hexagons. The legs are connected to the vertices of the hexagons;

- *TSSM robot (Triangular Simplified Symmetric Manipulator)* in which the mobile platform is triangular whereas the base is hexagonal. Two legs are connected on the same vertex of the triangle;
- *MSSM robot (Minimal Simplified Symmetric Manipulator)* in which the base and the mobile platform are triangular. Legs are mounted by pairs at both ends. The architecture forms an octahedron.

With six legs in parallel, there are five loops, and the application of equation [8.2] ($N = 6d - 6x5$) results in six degrees of freedom per leg (five passive and one active). The passive degrees of freedom can be distributed according to the combinations (0,5), (1,4) or (2,3). The (2,3) combination is the most popular one. It is composed of a universal joint (RR) and a spherical joint (RRR). The six degrees of freedom of the mobile platform are obtained by actuating each leg by either a prismatic joint (Figure 8.7) or a revolute joint (Figure 8.8). In the first case, the leg architecture is composed of (RR)-P-(RRR) joints, and in the second case, of R-(RR)-(RRR) joints.

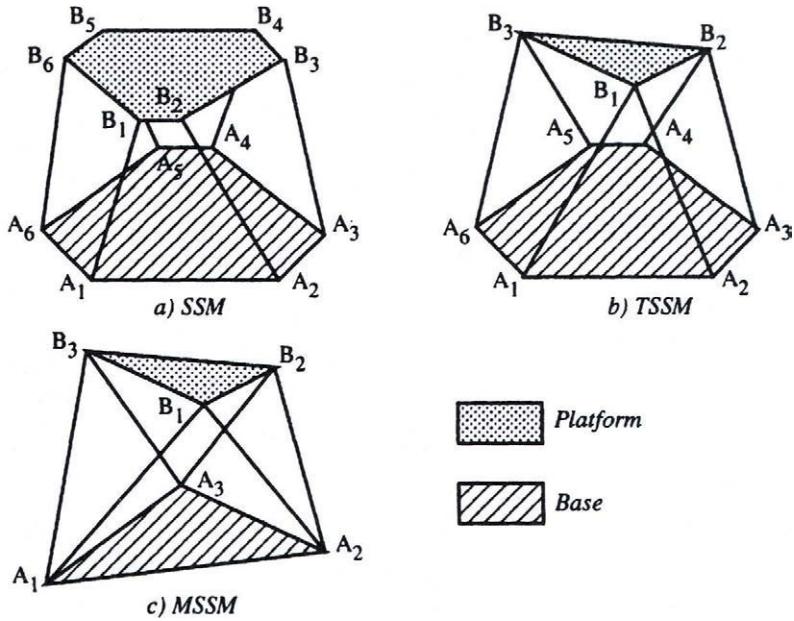

Figure 8.6. *SSM, TSSM and MSSM parallel robots*

Figure 8.9 presents a robot with a (0,5) combination for the passive joints. In this case, the leg orientation is fixed with respect to the base, whereas the mobile platform is connected to each leg through a five degree-of-freedom passive joint, a so-called C5 joint [Dafaoui 94]. The C5 joint is realized by a spherical joint fixed to

two perpendicular prismatic joints. The leg lengths are actuated by prismatic joints, giving for each leg a P-(RRRPP) architecture.

Note that we can find a six degree-of-freedom spatial robot with only three legs with R-R-P-(RRR) architecture as shown in Figure 8.7a. In this case, each leg has two active joints, namely the revolute joint, which is close to the base, and the prismatic joint. Such structure has been achieved on the so-called *Space robot* [Beji 97]. The application of equation [8.2] gives N = 6 for this structure.

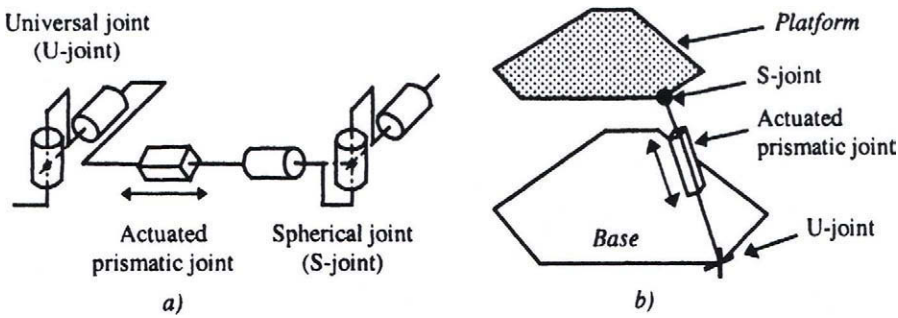

Figure 8.7. *(RR)-P-(RRR) architecture*

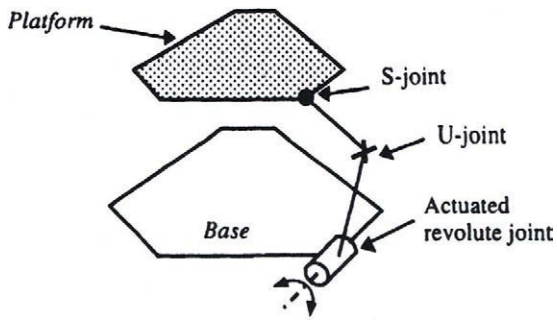

Figure 8.8. *R-(RR)-(RRR) architectures*

8.5.3. *The Delta robot and its family*

An interesting realization actually being implemented in several industrial applications is the Delta robot designed by Clavel [Clavel 89] (Figure 8.10a). This robot has four degrees of freedom, the fourth being fixed on the mobile platform and allowing the end-effector to rotate around the vertical axis. The moving platform always remains parallel to the base. It is connected to the base by three identical kinematic chains having a R-(RR)-(RR) architecture. The parallel chains are

actuated by the revolute joints, which are close to the base, using DC motors fixed to the base. With this architecture, the Delta has a very low inertia and can manipulate light pieces within a very short cycle time (typically, two pieces of 10g per second). This robot also presents the advantage of having a relatively large workspace. One can find in [Hervé 91], [Goudali 96] examples of robots derived from this architecture.

Pierrot [Pierrot 91b] has extended the Delta robot concept into a six degree-of-freedom robot, the *Hexa robot* (Figure 8.10b). The six actuators are fixed to the base and provide a speed of 8 m/s and an acceleration of 22 g to the mobile platform.

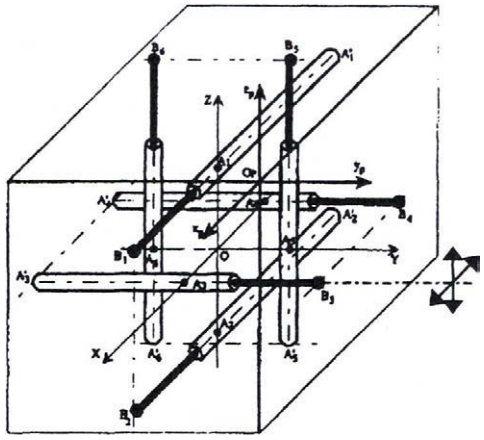

Figure 8.9. *Parallel robot with C5 joints [Dafaoui 94]*

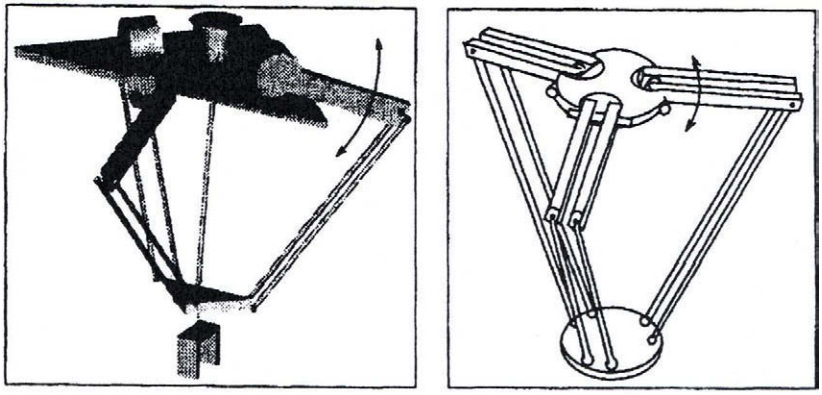

a) *b)*

Figure 8.10. *The Delta (a) and Hexa (b) robots (from [Clavel 89] and [Pierrot 91b] in [Merlet 00])*

8.6. Modeling the six degree-of-freedom parallel robots

In this section, we present the geometric and kinematic models of the Gough-Stewart parallel robots. The techniques developed in Chapter 7 for closed loop structures, namely the geometric description notations and the geometric and kinematic modeling methods can also be used for parallel robots. However, specific methods are usually more efficient. The proposed approach has direct relevance to the entire class of parallel robots such as the Delta robot [Clavel 89] and Hexa robot [Pierrot 91b].

8.6.1. *Geometric description*

We assume that the universal joints (U-joint) and the spherical joints (S-joint) are perfect, and that the prismatic joints are perfectly assembled. The centers of the U-joints and S-joints are denoted by A_i and B_i, for i = 1, ..., 6, respectively (Figure 8.11). Two coordinate systems need to be set up for the geometric description of a parallel structure: frame R_0 is attached to the base and frame R_m is attached to the mobile platform. They are defined as follows:

- A_1 is the origin of frame R_0, the x_0 axis is along A_1A_2, and the x_0y_0 plane is determined by A_1, A_2 and A_6;
- similarly, B_1 is the origin of frame R_m, the x_m axis is along B_1B_2, and B_1, B_2, B_6 are in the x_my_m plane.

The geometry of such a robot is described by:

- the (6x1) joint variable vector $\mathbf{q}$ representing the leg lengths A_iB_i for i = 1, ..., 6;
- the coordinates of the connection points A_i and B_i in frames R_0 and R_m respectively ($^0\mathbf{P}_{A_i}$ and $^m\mathbf{P}_{B_i}$ for i = 1, ..., 6). Note that the points A_i may not be necessarily in the same plane, nor the points B_i.

According to the definition of frames R_0 and R_m, we obtain:

$$^0P_{xA1} = {}^0P_{yA1} = {}^0P_{zA1} = {}^0P_{yA2} = {}^0P_{zA2} = {}^0P_{zA6} = 0$$
$$^mP_{xB1} = {}^mP_{yB1} = {}^mP_{zB1} = {}^mP_{yB2} = {}^mP_{zB2} = {}^mP_{zB6} = 0$$

where $^j\mathbf{P}_{P_i}$ denotes the position of a point P_i with respect to frame R_j:

$$^j\mathbf{P}_{P_i} = [\ {}^jP_{xP_i} \quad {}^jP_{yP_i} \quad {}^jP_{zP_i}\ ]^T$$

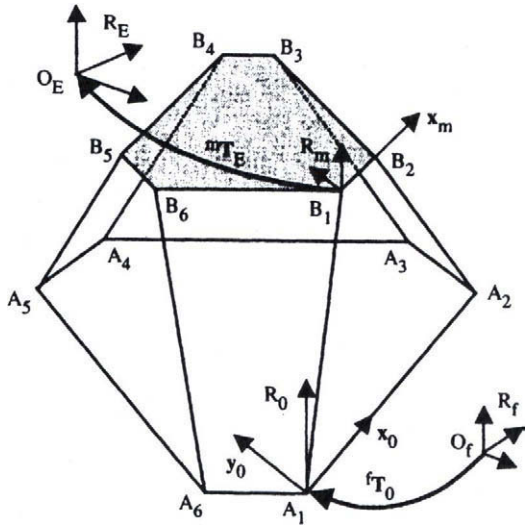

Figure 8.11. *Geometric notations*

Thus, the robot is described by 24 constant parameters that may be not zero.

In order to describe the location of the robot base frame R_0 with respect to the environment world reference frame R_f, we use the matrix $\mathbf{Z} = {}^fT_0$. Similarly, to define a general end-effector frame R_E with respect to frame R_m, we use the matrix $\mathbf{E} = {}^mT_E$. Consequently, the location of the end-effector frame relative to the world reference frame is:

$$^fT_E = \mathbf{Z}\,{}^0T_m(q)\,\mathbf{E} \qquad [8.5]$$

The coordinates of a connection point A_i relative to frame R_f are given by:

$$\begin{bmatrix} {}^fP_{Ai} \\ 1 \end{bmatrix} = {}^fT_0 \begin{bmatrix} {}^0P_{Ai} \\ 1 \end{bmatrix} = \mathbf{Z} \begin{bmatrix} {}^0P_{Ai} \\ 1 \end{bmatrix} \qquad [8.6]$$

The coordinates of the connection point B_i relative to frame R_E are:

$$\begin{bmatrix} {}^EP_{Bi} \\ 1 \end{bmatrix} = {}^ET_m \begin{bmatrix} {}^mP_{Bi} \\ 1 \end{bmatrix} = \mathbf{E} \begin{bmatrix} {}^mP_{Bi} \\ 1 \end{bmatrix} \qquad [8.7]$$

The matrices **Z** and **E** can be defined arbitrarily; therefore, six independent parameters are needed to define each of them.

To conclude, we can define the end-effector frame with respect to the reference frame using 42 geometric parameters (36 constant geometric parameters and 6 joint variables representing the leg lengths). The 36 constant parameters can be defined either by ${}^{f}\mathbf{P}_{A_i}$ and ${}^{E}\mathbf{P}_{B_i}$, or by the 24 coordinates of ${}^{0}\mathbf{P}_{A_i}$ and ${}^{m}\mathbf{P}_{B_i}$, which may be not zero, and the matrices $\mathbf{E}$ and $\mathbf{Z}$. These parameters allow us to calculate the kinematic and geometric models. The second set of parameters is interesting when calibrating the geometric parameters using autonomous methods and when developing symbolic geometric or kinematic models.

8.6.2. *Inverse geometric model*

The inverse geometric model (IGM) provides the joint variables $\mathbf{q}$ corresponding to a given location ${}^{f}\mathbf{T}_{E}$ of the end-effector. It is represented by:

$$\mathbf{q} = \mathrm{IGM}({}^{f}\mathbf{T}_{E}) \qquad [8.8]$$

with:

$$\mathbf{q} = [q_1 \ \cdots \ q_6]^T \qquad [8.9]$$

Since ${}^{E}\mathbf{P}_{B_i}$ and ${}^{f}\mathbf{T}_{E}$ are known, we can compute the coordinates of the connection points B_i with respect to the reference frame by the following relation:

$$\begin{bmatrix} {}^{f}\mathbf{P}_{B_i} \\ 1 \end{bmatrix} = {}^{f}\mathbf{T}_{E} \begin{bmatrix} {}^{E}\mathbf{P}_{B_i} \\ 1 \end{bmatrix} \qquad [8.10]$$

The prismatic variable q_i is equal to the distance between the connection points A_i and B_i:

$$q_i^2 = ({}^{f}\mathbf{P}_{B_i} - {}^{f}\mathbf{P}_{A_i})^T ({}^{f}\mathbf{P}_{B_i} - {}^{f}\mathbf{P}_{A_i}) = ({}^{f}\mathbf{A}_i\mathbf{B}_i)^T {}^{f}\mathbf{A}_i\mathbf{B}_i \qquad [8.11]$$

This equation shows that the IGM of the Gough-Stewart parallel robot is unique and can be easily determined. The equations giving the leg lengths are independent and can be computed in parallel [Merlet 00]. This result is not general for all parallel robots. For example, the IGM of a three degree-of-freedom spatial robot (Figure 8.5) is not unique: for a given position of the endpoint, there are four possible solutions for the leg lengths [Gosselin 88].

8.6.3. *Inverse kinematic model*

The inverse kinematic model (IKM) provides the actuated joint velocity $\dot{\mathbf{q}}$ corresponding to a given kinematic screw of the end-effector. It is denoted by:

$$\dot{\mathbf{q}} = {}^{f}\mathbf{J}_{E}^{-1}\begin{bmatrix} {}^{f}\mathbf{V}_{E} \\ {}^{f}\boldsymbol{\omega}_{E} \end{bmatrix} \qquad [8.12]$$

where ${}^{f}\mathbf{V}_{E}$ is the linear velocity of O_E, origin of frame R_E, and ${}^{f}\boldsymbol{\omega}_{E}$ is the angular velocity of the end-effector.

The inverse differential model can be defined by:

$$\mathbf{dq} = {}^{f}\mathbf{J}_{E}^{-1}\begin{bmatrix} {}^{f}\mathbf{dP}_{E} \\ {}^{f}\boldsymbol{\delta}_{E} \end{bmatrix} \qquad [8.13]$$

The computation of ${}^{f}\mathbf{J}_{E}^{-1}$ is obtained by projecting the velocity of the connection points of the mobile platform onto the leg directions. Let ${}^{f}\mathbf{V}_{B_i}$ be the velocity of the point B_i with respect to frame R_E; hence we can write:

$${}^{f}\mathbf{V}_{B_i} = {}^{f}\mathbf{V}_{E} + {}^{f}\mathbf{B}_{i}\mathbf{O}_{E} \times {}^{f}\boldsymbol{\omega}_{E} \qquad [8.14]$$

Thus, the joint velocity $\dot{q}_i$, for $i = 1, \ldots, 6$, can be computed by:

$$\dot{q}_i = {}^{f}\mathbf{u}_{i}^{T}\,{}^{f}\mathbf{V}_{B_i} \qquad [8.15]$$

where $\mathbf{u}_i$ is the unit vector along the i^{th} leg:

$$\mathbf{u}_i = \frac{\mathbf{A}_i\mathbf{B}_i}{\|\mathbf{A}_i\mathbf{B}_i\|} = \frac{\mathbf{A}_i\mathbf{B}_i}{q_i} \qquad [8.16]$$

Combining equations [8.14] and [8.15] leads to:

$$\dot{q}_i = {}^{f}\mathbf{u}_{i}^{T}\,{}^{f}\mathbf{V}_{E} + {}^{f}\mathbf{u}_{i}^{T}\,({}^{f}\mathbf{B}_{i}\mathbf{O}_{E} \times {}^{f}\boldsymbol{\omega}_{E}) \qquad [8.17]$$

which can be rewritten as:

$$\dot{q}_i = {}^{f}\mathbf{u}_{i}^{T}\,{}^{f}\mathbf{V}_{E} + ({}^{f}\mathbf{u}_{i} \times {}^{f}\mathbf{B}_{i}\mathbf{O}_{E})^{T}\,{}^{f}\boldsymbol{\omega}_{E} \qquad [8.18]$$

Consequently, the i^{th} row of the inverse Jacobian matrix is given by:

$$\mathbf{L}_i = [\ {}^f\mathbf{u}_i^T \quad ({}^f\mathbf{u}_i \times {}^f\mathbf{B}_i\mathbf{O}_E)^T\ ] \qquad [8.19]$$

and finally:

$${}^f\mathbf{J}_E^{-1} = \begin{bmatrix} {}^f\mathbf{u}_1{}^T & ({}^f\mathbf{u}_1 \times {}^f\mathbf{B}_1\mathbf{O}_E)^T \\ {}^f\mathbf{u}_2{}^T & ({}^f\mathbf{u}_2 \times {}^f\mathbf{B}_2\mathbf{O}_E)^T \\ \cdots & \cdots \\ {}^f\mathbf{u}_6{}^T & ({}^f\mathbf{u}_6 \times {}^f\mathbf{B}_6\mathbf{O}_E)^T \end{bmatrix} \qquad [8.20]$$

The direct kinematic model is obtained by inverting equation [8.20].

8.6.4. *Direct geometric model*

The direct geometric model (DGM) provides the location of the end-effector corresponding to a given joint configuration $\mathbf{q}$. It is written as:

$${}^f\mathbf{T}_E = \mathrm{DGM}(\mathbf{q}) \qquad [8.21]$$

8.6.4.1. *Closed-form solution*

The solution of the DGM is relatively complicated to derive. In general, for a given set of joint variables, the mobile platform can take several different locations.

In order to find an analytical solution to the general six degree-of-freedom Gough-Stewart parallel robot, some authors propose to incorporate additional position sensors on some selected passive joints [Cheok 93], [Merlet 93], [Baron 94], [Han 95], [Tancredi 95].

Recently, Husty [Husty 96] presented a method giving all the DGM solutions of a general Gough-Stewart parallel robot. It is based on the resolution of a 40^{th} degree polynomial in a single variable. The other variables are then uniquely determined. Some of these solutions may be complex numbers. However, this method does not give the maximum number of real solutions. It does not indicate if the solutions can be reached from a given configuration without crossing a singularity or after having crossed a singularity. The Husty algorithm confirms Raghavan's work [Raghavan 91] and Lazard's work [Lazard 92] that found the same number of solutions by numerical methods. In [Dietmaier 98], we find an example of a robot with 40 real solutions.

Closed-form solutions of the DGM have been proposed for the special (non-exhaustive) following architectures:

1) TSSM architectures (Figure 8.6b): the notion of equivalent mechanism allows us to derive the direct geometric model of spatial robots with a triangular platform. This approach has been used by Hunt [Hunt 83] and [Charentus 90] to compute the DGM of TSSM architectures. The problem is reduced to solving three equations in three unknowns, which are the rotation angles of these triangles about the base.

Indeed, in the TSSM architecture, each of the triangular faces $A_1A_2B_1$, $A_3A_4B_2$ and $A_5A_6B_3$ can only rotate around the axes A_1A_2, A_3A_4 and A_5A_6 respectively. This results in the equivalent mechanism shown in Figure 8.12.

The three equivalent segments r_1, r_2 and r_3 sweep three circles in the space and it can be shown that the solution of the DGM is given by an 8^{th} degree polynomial. Thus, the number of possible configurations for a given vector $\mathbf{q}$ is 16 while taking into account the symmetry of solutions with respect to the base.

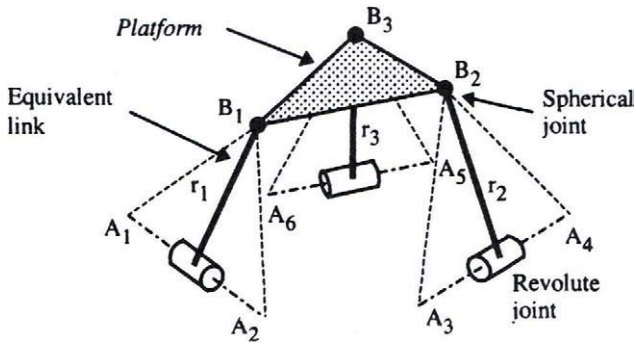

Figure 8.12. *Equivalent TSSM architecture with three rigid triangular faces*

2) Gough-Stewart robots with five collinear connection points: Zhang and Song [Zhang 92] showed that the DGM of such a parallel robot has an analytical solution (4^{th} degree polynomial at most) if the connection points of five legs on either the base or the platform are collinear. Such structure decouples a rotational degree of freedom of the platform from the other five (Figure 8.13). The number of solutions is eight, four with P_{z_m} positive, the other four with P_{z_m} negative. A study of the duality of this architecture with a six degree-of-freedom serial robot having a spherical wrist can be found in [Khalil 96c].

3) 4-4 Gough-Stewart robots: [Lin 92] gives the polynomial solution of the DGM of a Gough-Stewart robot in which two pairs of connection points of the mobile platform are coincident, as well as two pairs of connection points of the base plate. The connection points of the base lie on one plane and those of the mobile platform lie on another one. The solution is given by a 12^{th} degree polynomial at most.

4) 5-4 Parallel robots: Innocenti and Parenti-Castelli [Innocenti 93] give the solution of a Gough-Stewart robot in which two connection points of the base are coincident as well as two pairs of connection points of the mobile platform (Figure 8.14). The solution is given by a 24^{th} degree polynomial in one variable, the other variables being uniquely determined. A similar result has been obtained for the 5-5 robot [Innocenti 95].

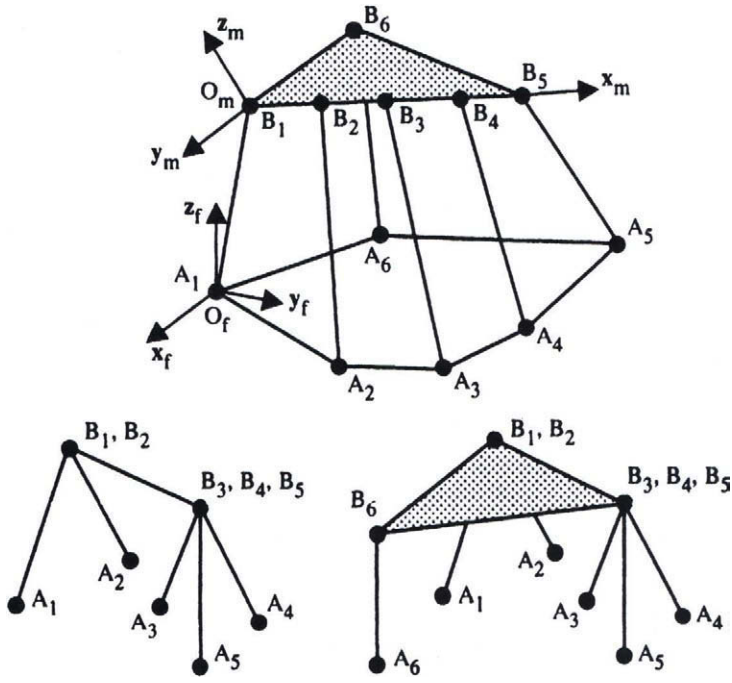

Figure 8.13. *Architectures with five collinear connection points*

5) Gough-Stewart robot with similar base and platform: it has been shown that all the joint variables can be obtained from linear or quadratic equations when the connection points of the base lie on one plane and those of the mobile platform lie on another one, and the form of the base and the mobile platform are similar (same form but different sizes). The number of solutions is 16 [Lee 93].

6) Gough-Stewart robot with three coincident connection points on the base as well as on the mobile platform: this so-called $(3\text{-}1\text{-}1\text{-}1)^2$ robot has eight solutions that can be analytically computed [Bruyninckx 98].

7) Six degree-of-freedom parallel robot with a C5 joint: it can be shown that such an architecture (Figure 8.9), which has a very small workspace, has a unique solution for both the DGM and the IGM [Dafaoui 94].

8) Delta family: the DGM may be obtained by solving a 2^{nd} degree polynomial [Pierrot 91a].

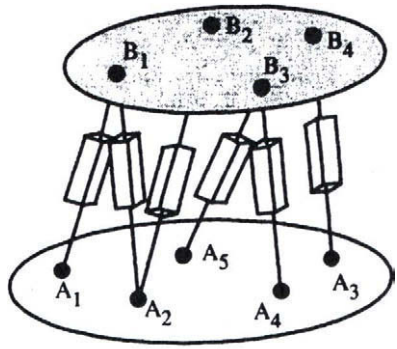

Figure 8.14. *Six degree-of-freedom (5-4) parallel robot*

8.6.4.2. *Numerical solution*

Practically, we can use the inverse differential model to compute a numerical solution of the DGM in an iterative manner. For a given $\mathbf{q}^d$, the algorithm is as follows:

- from an initial location ${}^fT_E^c$ (random or current location) of the mobile platform, compute the corresponding joint variables $\mathbf{q}^c$ using the IGM;
- compute the difference between $\mathbf{q}^d$ and the current $\mathbf{q}^c$: $\mathbf{dq} = \mathbf{q}^d - \mathbf{q}^c$. If $\mathbf{dq}$ is small enough, ${}^fT_E^d = {}^fT_E^c$, then stop the computation;
- using equation [8.20], compute the inverse Jacobian matrix ${}^fJ_E^{-1}$;
- compute numerically the direct Jacobian matrix ${}^fJ_E = ({}^fJ_E^{-1})^+$;
- compute the position error ${}^fdP_E$ and the orientation error ${}^f\delta_E = \theta\,\mathbf{u}$ (where $\mathbf{u}$ is a unit vector) corresponding to $\mathbf{dq}$ by using the relation:

$$\begin{bmatrix} {}^fdP_E \\ {}^f\delta_E \end{bmatrix} = {}^fJ_E\,\mathbf{dq} \qquad [8.22]$$

- update the current position and orientation of the mobile platform:

$$ {}^{f}\mathbf{T}_{E}^{c} = \begin{bmatrix} {}^{f}\mathbf{A}_{E}^{c} & {}^{f}\mathbf{P}_{E}^{c} \\ 0 \; 0 \; 0 & 1 \end{bmatrix} \qquad [8.23] $$

with:

$$ {}^{f}\mathbf{P}_{E}^{c} = {}^{f}\mathbf{P}_{E}^{c} + {}^{f}\mathbf{dP}_{E} \qquad [8.24] $$

$$ {}^{f}\mathbf{A}_{E}^{c} = \mathbf{rot}(\mathbf{u}, \theta)\, {}^{f}\mathbf{A}_{E}^{c} \qquad [8.25] $$

- return to the first step.

This algorithm is efficient and can be computed in real time.

8.7. Singular configurations

Singular configurations of parallel robots are particular configurations at which the robot loses its natural rigidity. At these configurations, one or more degrees of freedom of the platform become uncontrollable. From such an initial configuration, the mobile platform moves toward an equilibrium location under the effect of the wrench applied to the mobile platform, for example, under the effect of the gravity loading of the platform and the manipulated load. Such a motion is due to the passive joints, while the actuated joints are fixed (§ 7.11).

Mathematically, the singular configurations can be determined by analyzing the static equilibrium of the robot. Let Γ be the vector of the joint torques and let $\mathbb{f}$ be the static wrench applied to the mobile platform. The static equilibrium of the robot is defined as (§ 5.9.2):

$$ \mathbb{f} = (\mathbf{J}^{-1})^{T} \Gamma \qquad [8.26] $$

In order to maintain the equilibrium of the robot, the inverse Jacobian matrix has to be regular, such that for a given wrench $\mathbb{f}$, there is a corresponding finite joint torque vector Γ.

The singular configurations can be determined by analyzing the rank of the matrix $\mathbf{J}^{-1}$. From equation [8.12], we can deduce that at a singular configuration, a motion in the null space of $\mathbf{J}^{-1}$ is possible even though $\dot{\mathbf{q}} = \mathbf{0}$ (§ 7.11). From equation [8.26], we see that at a singular configuration the motor torques Γ can be infinity, which may damage the robot. Thus, parallel robots should be designed without singularities in the reachable space. This can be attained by good selection of joint geometric parameters and joint limits, and even by providing the robot with redundant actuators on some passive joints [Merlet 00].

Merlet [Merlet 89] proposed to study the singularity using another interesting geometric method based on Grassmann manifolds.

The analysis of singularities has led some authors to propose design-related rules in order to avoid singular structures. Ma and Angeles [Ma 91] demonstrated that the inverse Jacobian matrix is singular throughout the whole workspace of the robot if the mobile platform and the base are made of regular and similar polygons with six connecting points. Such singularity is called *architecture singularity* and the corresponding architecture is called *singular architecture*. Figure 8.15 depicts this architecture, the mobile platform and the base being homothetical.

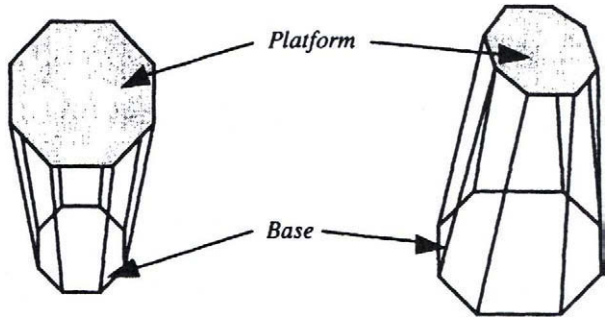

Figure 8.15. *Singular architectures*

8.8. Conclusion

In this chapter, we have presented the geometric and kinematic models of Gough-Stewart structures, which are considered to be representative of parallel robots. We have shown that the techniques developed for serial robots are often not appropriate and special approaches have to be used. The IGM and IKM are simple and straightforward to derive. On the contrary, the analytical DGM is not easy to compute in the general case since 40 solutions are possible. It was observed that merging some of the connection points on the platform or the base or both, by groups of two or three, simplifies the closed-form solution of the problem and also reduces the maximum number of possible solutions.

In addition, the numerical solution of the DGM can be used in most practical applications where only one real solution is required provided that a good initial location is available.